Journal of Modern Optics
Vol. 52, No. 16, 10 November 2005, 2381–2390

Taylor & Francis
Taylor & Francis Group

EIT and diffusion of atomic coherence

I. NOVIKOVA*†, Y. XIAO†, D. F. PHILLIPS† and R. L. WALSWORTH†‡
†Harvard-Smithsonian Center for Astrophysics, Cambridge, MA, 02138, USA
‡Department of Physics, Harvard University, Cambridge, MA, 02138, USA

(*Received 15 February 2005; in final form 25 May 2005*)

We study experimentally the effect of diffusion of Rb atoms on electromagnetically induced transparency (EIT) in a buffer gas vapour cell. In particular, we find that diffusion of atomic coherence in and out of the laser beam plays a crucial role in determining the EIT resonance lineshape and the stored light lifetime.

In this paper we address an important issue for electromagnetically induced transparency (EIT) [1, 2] and stored light [3, 4] in alkali vapour cells (i.e. warm atoms with buffer gas): the practical role of the diffusion of atomic coherence in and out of the laser fields that prepare and probe the atoms. EIT occurs in a three-level Λ-system in which two coherent electromagnetic fields (the probe and control fields) are in two-photon Raman resonance with two atomic ground-state sublevels, as shown in figure 1(*a*). The atoms are optically pumped into a 'dark state', a coherent superposition of the two ground-state sublevels which is decoupled from the optical fields. Typically, a buffer gas is included to restrict the motion of the EIT atoms and thus lengthen the atomic interaction time with the laser fields [5–8]; and also to pressure broaden the electronic excited state so as to allow co-propagating probe and control fields that interact with most of the atoms despite Doppler broadening [9, 10].

In this regime, atomic diffusion is important, yet rather subtle to model effectively. To date EIT models have treated diffusion phenomenologically, by assuming a simple homogeneous decay of the ground state coherence characterized by the timescale τ_D of the lowest order diffusion mode across the laser beam [5, 8, 11]. Some recent experiments have seen indications of the inadequacy of this simple approach [12–14]. Here we report experiments that show that diffusion of atomic coherence in and out of the laser beam (i.e. from the region illuminated by the optical fields to the surrounding, unilluminated region, and then back into the laser beam) plays a crucial role in determining the EIT resonance lineshape and the lifetime of stored light. As described below, we observed a narrow central peak in the EIT resonance (much narrower than $1/\tau_D$) due to the contribution of atoms diffusing

*Corresponding author. Email: i.novikova@osa.org

Journal of Modern Optics
ISSN 0950–0340 print/ISSN 1362–3044 online © 2005 Taylor & Francis
http://www.tandf.co.uk/journals
DOI: 10.1080/09500340500275637

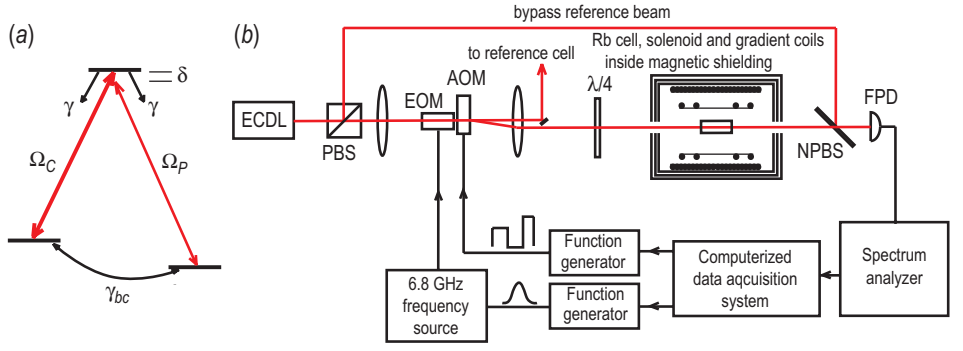

Figure 1. (*a*) Simplified three-level Λ system; (*b*) schematic of the experimental setup (see text for abbreviations).

in and out of the laser beam. We then eliminated this narrow peak by applying transverse gradients in the longitudinal magnetic field to decohere atoms that diffuse well out of the laser beam. Finally, we measured the influence of atomic coherence diffusion on light pulses that have been stored in the atomic ensemble using a dynamic EIT technique.

1. Experimental setup

As shown in figure 1, we employed an external cavity diode laser (ECDL) tuned to the D_1 line of ^{87}Rb. The total available laser power was about 13 mW. We used a polarizing beam splitter (PBS) to create a bypass reference beam. We modulated the phase of the main laser field at 6.835 GHz (near the ^{87}Rb ground-state hyperfine splitting) using an electro-optical modulator (EOM), so that approximately 2% of the total laser power was transferred to each first order sideband. All three optical fields then passed through an acousto-optical modulator (AOM), shifting the frequencies of all fields by +80 MHz. We tuned the laser such that the main carrier frequency field was resonant with the $5S_{1/2}F = 2 \rightarrow 5P_{1/2}F' = 2$ transition of ^{87}Rb; in this case the +1 sideband was resonant with the $5S_{1/2}F = 1 \rightarrow 5P_{1/2}F' = 2$ transition. We neglected any influence of the far-detuned −1 sideband.

Before entering the Rb vapour cell the laser beam was weakly focused to a 0.8 mm diameter spot and circularly polarized using a quarter-wave plate ($\lambda/4$). We mounted the cylindrical glass cell, containing isotopically enriched ^{87}Rb and either 5 torr or 100 torr Ne buffer gas ($D = 35.7\,\mathrm{cm}^2/\mathrm{s}$ and $D = 1.78\,\mathrm{cm}^2/\mathrm{s}$ respectively [15, 16]), inside a three-layer magnetic shield, which reduced stray magnetic fields to less than 100 μG over the interaction region. A solenoid inside the magnetic shields provided a weak bias magnetic field B_0 ($\leq$100 mG). We controlled the temperature of the cell to ±0.2 K using a blown-air oven. For the EIT lineshape measurements we kept the temperature low enough (45°C for the 5 torr Ne cell, and 55°C for the 100 torr Ne cell) to ensure an optically thin Rb vapour; for stored light experiments we operated with the cell at 65°C to provide significant pulse delay and storage.

After traversing the cell, the laser beam was combined with the bypass reference beam on a non-polarizing beam-splitter (NPBS) and sent to a fast photodetector (FPD). Since the frequency of the reference field was 80 MHz lower than the control field, we detected the +1 sideband by measuring the amplitude of the beat note at 6.915 GHz using a microwave spectrum analyser.

2. Gradient coils

Pulsed magnetic field gradients are a well-established tool in NMR for imaging (MRI) and for measuring diffusion and coherent flow in liquids and gases. In our experiment we used a standard gradient coil design (see figure 2) [17, 18] to produce a controllable linear gradient of the longitudinal magnetic field in the transverse direction: $\partial B_z/\partial x$ up to 40 mG/(cm · A), with excellent linearity at the centre of the coils.

Note that away from the coil centre a transverse magnetic field is also created such that $\partial B_z/\partial x = \partial B_x/\partial z$. In traditional high-field NMR applications, the effect of the transverse magnetic field is negligible. In our experiment the weak bias magnetic field B_0 limits the gradient strength we can use without distorting the EIT resonance: $\partial B_x/\partial z \cdot L/2 \ll \sqrt{2}B_0$, where L is the length of the cell.

3. Steady-state EIT in buffer gas cells

Figure 3 shows a typical example of the measured EIT lineshape (i.e. the probe field transmission as a function of two-photon detuning) for the 5 torr Ne cell and no applied magnetic fields. Note the sharp, narrow peak on-resonance. Also note that the FWHM is significantly narrower that $1/\pi\tau_D \approx 26$ kHz [5, 11], i.e. the linewidth set naively by single-pass diffusion across the laser beam. The shape of this EIT resonance is clearly not the Lorentzian function predicted by simple three-level EIT theory [10]:

$$|\Omega_P^{(\mathrm{out})}|^2 \propto 1 - \frac{\gamma_{bc}\gamma|\Omega_C|^2 + \delta^2\gamma^2}{|\Omega_C|^4 + \delta^2\gamma^2} \tag{1}$$

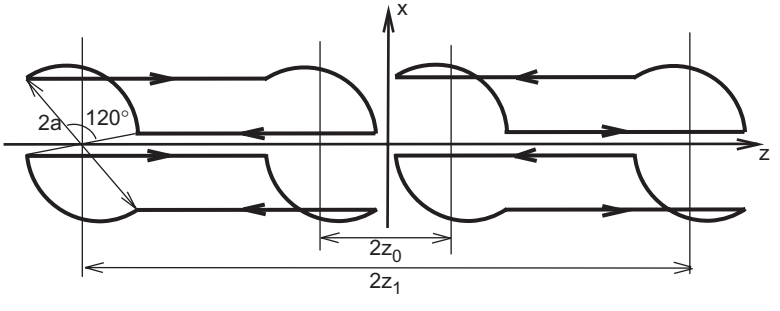

Figure 2. Schematic of the magnetic field gradient coils. Dimensions are: $z_0 = 2.4$ cm, $z_1 = 16.2$ cm, $a = 6.4$ cm, chosen to optimize the linearity of the gradient field $\partial B_z/\partial x$ [17, 18].

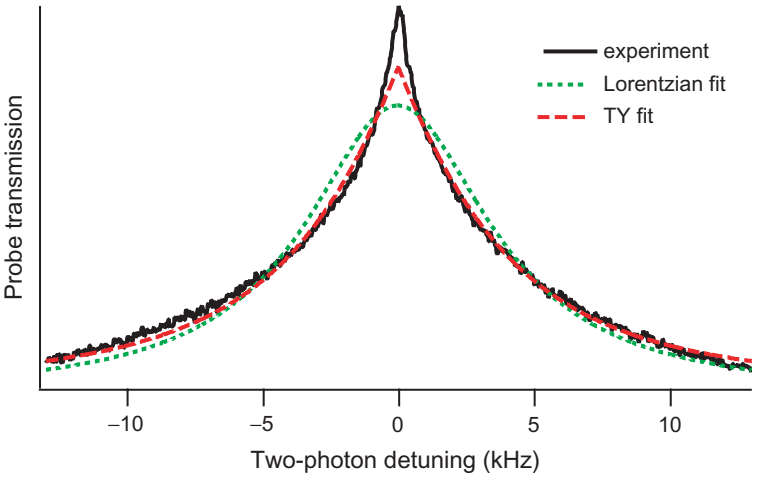

Figure 3. Measured intensity of the probe field transmission (EIT) as a function of two-photon detuning δ. Also shown are the best Lorentzian fit (equation 1) and 'TY-fit' (equation 2), which assumes spatially inhomogeneous power broadening of the EIT lineshape as determined by a Gaussian distribution of the transverse laser intensity profile. Total laser power $\approx 50\,\mu W$.

where Ω_P and Ω_C are the probe and control field Rabi frequencies, $|\Omega_P^{(out)}|^2$ is proportional to the probe field transmitted intensity, δ is the two-photon detuning, and γ and γ_{bc} are respectively the excited-state and ground-state coherence relaxation rates (see figure 1*a*).

Recent extensions of three-level EIT theory have considered the effect of atomic motion in a laser beam with a Gaussian intensity profile in the transverse direction. In the regime of high buffer gas pressure and moderately high laser intensity, the motion of alkali atoms across the laser beam is assumed to be slower than the excited and ground-state relaxation rates, and the atomic coherence is assumed to adjust instantaneously to the light intensity at each point of the laser beam. Thus atoms in the centre of the laser beam, where the laser intensity is maximum, have greater power broadening than atoms in the wings. For a Gaussian laser intensity profile, the probe field transmission lineshape is then found to be [19]:

$$|\Omega_P^{(out)}|^2 \propto 1 - \frac{\delta\gamma}{|\Omega_C|^2}\arctan\frac{|\Omega_C|^2}{\delta\gamma} \tag{2}$$

which we refer to as the 'TY-fit'. In the regime of low buffer gas pressure and very low light intensity, there is negligible power broadening and the EIT lineshape is calculated to be [20]:

$$|\Omega_P^{(out)}|^2 \propto e^{-|\delta\cdot t_{tr}|} \tag{3}$$

where $t_{tr} = 2r/\langle v\rangle$ is the average alkali atom transit time through the laser beam, and $\langle v\rangle$ is the average thermal radial velocity of the alkali atoms. Interestingly, the lineshapes described by equations (2) and (3) are very similar for typical conditions

for Rb vapour EIT, despite being obtained in very different limits. In figure 3 we plot the best Lorentzian fit (equation 1) and TY-fit (equation 2), which is more relevant to our experimental conditions. The Lorentzian fit provides a poor approximation to our measurements; the TY-fit is superior to the Lorentzian fit, but it fails to reproduce the sharp structure on resonance.

The observed EIT lineshape may be understood if we assume that the diffusion of Rb atoms in and out of the laser beam creates a broad range of interaction times rather than a single average diffusion time τ_D. That is, we must account not only for atoms that diffuse once through the laser beam and then decohere (never return), but also those that diffuse out of the laser beam and return, and thus interact with the laser fields multiple times. For these returning atoms the interaction with the optical fields resembles a Ramsey separated oscillatory field experiment, with significant coherent evolution 'in the dark', leading to much narrower EIT resonances.

To better characterize the sharp central peak of the EIT resonance, we employed phase-sensitive detection. We used audio-frequency modulation of the 6.8 GHz synthesizer ($f_m \approx 150$ Hz), and detected changes in the laser transmission using a slow photodetector and lock-in amplifier. Figure 4 shows EIT resonance measurements made both with a spectrum analyser (covering the entire resonance) and phase-sensitive detection (restricted to the narrow centre of the resonance). For both the 5 torr and 100 torr Ne cell, we measured the spectral width of the narrow central EIT peak to be ≤ 500 Hz, and to be largely insensitive to laser power, which is consistent with the central peak reflecting coherent atomic evolution 'in the dark'.

To test the hypothesis that atoms diffusing in and out of the laser beam contribute significantly to the EIT lineshape (particularly the sharp central peak), we measured the EIT resonance in the presence of a linear transverse gradient in the longitudinal magnetic field $\partial B_z/\partial x$, using the gradient coils described above. For these measurements we also applied a uniform longitudinal field ($B_0 = 80$ mG) which splits the Rb ground-state Zeeman sublevels, and makes negligible the effects of the transverse component of the magnetic field created by the gradient coils (for $\partial B_z/\partial x \leq 4$ mG/cm). We studied EIT formed on the ground-state $m = 1$ Zeeman sublevels (i.e. coherence between the $F = 1$, $m_F = 1$ and $F = 2$, $m_F = 1$ levels). The associated transition frequency between those levels has a gyromagnetic ratio $\approx$1.4 MHz/G. Therefore, $\partial B_z/\partial x$ induces an inhomogeneous broadening to the EIT coherence; and for suitable magnitudes of this gradient, the broadening across the laser beam waist ($\approx$0.8 mm) can be small compared to the narrow central peak, while the larger magnetic field deviation outside the laser beam causes most atoms to decohere if they diffuse out of and then back in the laser field.

Figure 5 shows measured EIT resonances at several gradient strengths. For stronger gradients, the central peak becomes less sharp, and the TY-fit of the EIT lineshape is improved, which is consistent with diffusion-induced Ramsey narrowing being destroyed by gradient field induced decoherence of atoms that diffuse out of the laser beam.

Figure 6 illustrates the greater dependence on applied gradient of the spectral width of the central EIT peak for the 5 torr Ne cell, in comparison to

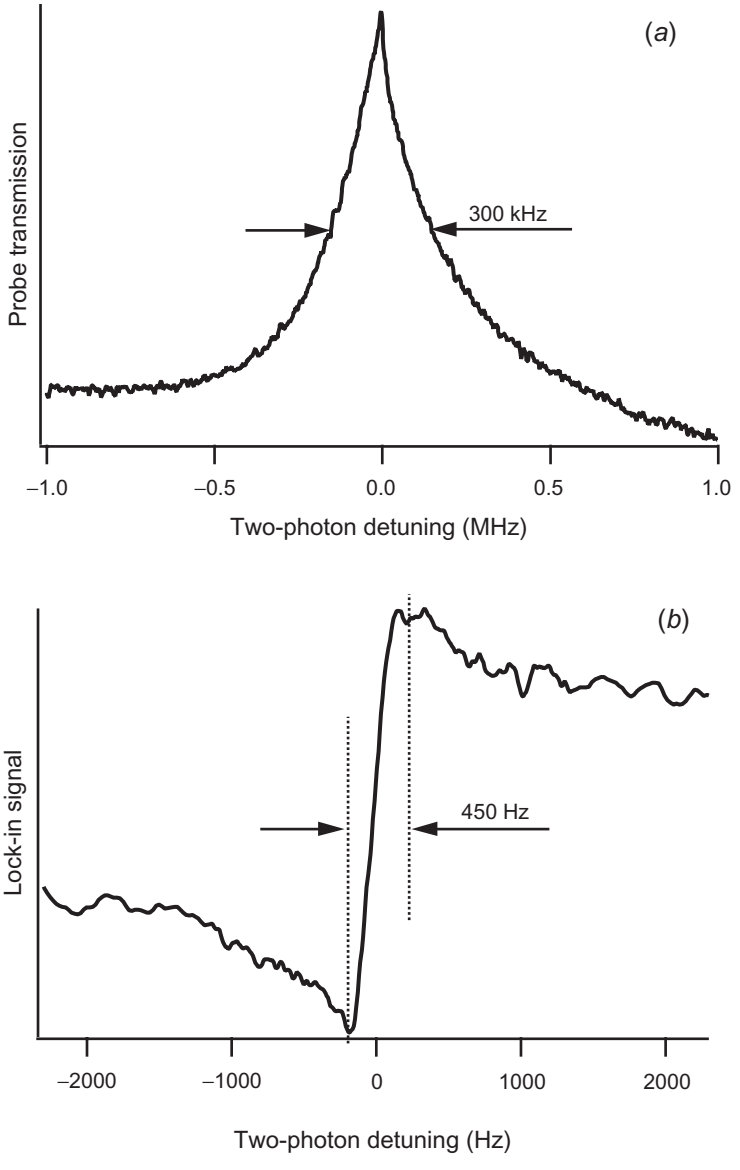

Figure 4. EIT resonance observed (*a*) with spectrum analyser and (*b*) using phase-sensitive detection. Both measurements are made in a 5 torr Ne cell at total laser power of 800 μW.

the 100 torr Ne cell. These measurements are also consistent with diffusion-induced Ramsey narrowing, which would be more thoroughly inhibited by the applied magnetic field gradient for the more rapid Rb diffusion in the 5 torr Ne cell. Modelling and quantitative analysis of these diffusion effects is reported in [22].

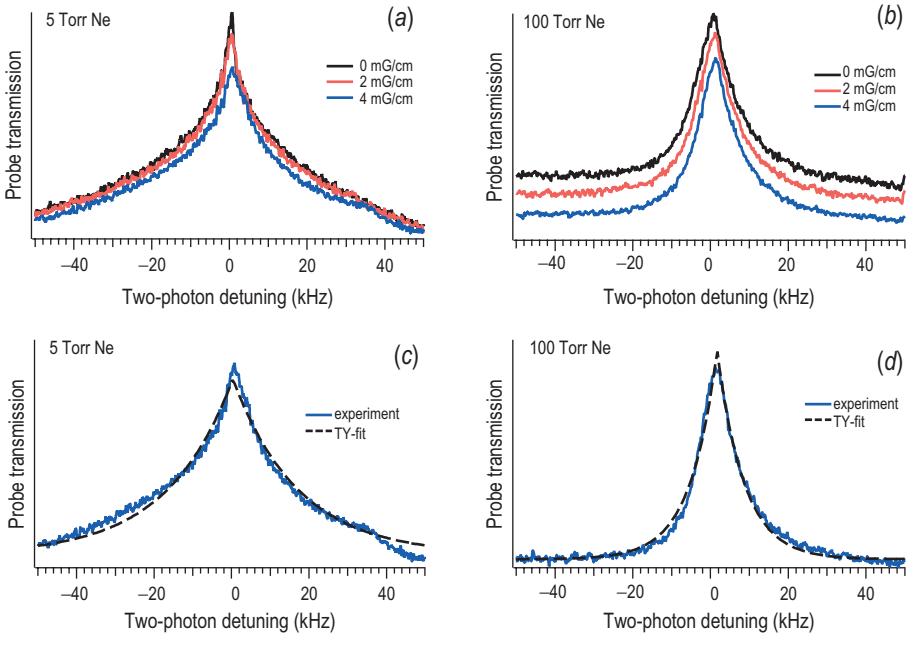

Figure 5. Modification of EIT resonance with applied magnetic field gradients for (*a*) 5 torr Ne cell and (*b*) 100 torr Ne cell. Bias magnetic field is $B_0 \approx 132$ mG, total laser power is $\approx 100\,\mu$W. Comparison of measured EIT resonance for 4 mG/cm gradient with TY-fit (equation 2) for (*c*) 5 torr Ne cell and (*d*) 100 torr Ne cell.

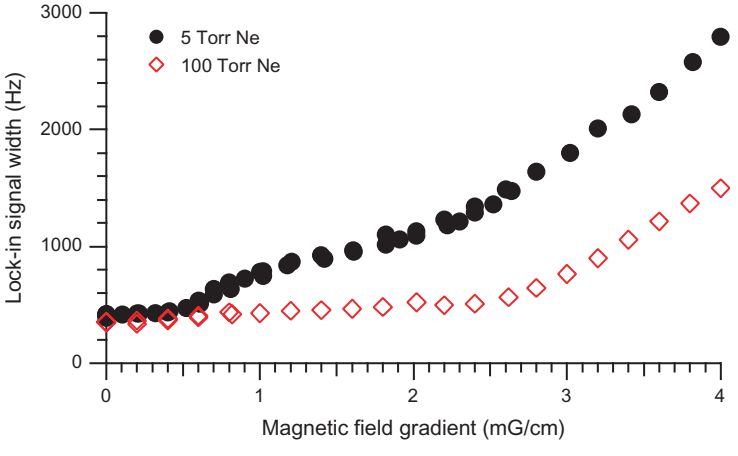

Figure 6. Broadening of the EIT central peak with applied magnetic field gradient measured with phase-sensitive detection, for both the 5 torr Ne and the 100 torr Ne buffer gas cells. Bias magnetic field is $B_0 \approx 80$ mG, total laser power $\approx 20\,\mu$W.

4. Stored light in a buffer gas cell

Under EIT conditions, the strength of the control field determines the coherent coupling between the probe field and the ground-state atomic coherence and thus the group velocity of probe pulse propagation through the medium [21]. Appropriate variation of the control field allows storage of the probe pulse in the form of an atomic ensemble coherence [3, 4]. In realistic atomic systems, the maximum storage time is determined by the atomic coherence lifetime, including the effect of coherence diffusion.

To avoid large additional absorption and pulse reshaping, the bandwidth of the probe pulse should be less than the sharp peak observed in the static probe field transmission [23]. We employed a Gaussian waveform for the probe pulse with a full width of 1 ms, which experienced a group delay $\approx$450 μs for a control field power of 50 μW. This delay is not great enough to trap the entire probe pulse inside the atomic vapour cell ($L = 7$ cm). We typically stored about half the Gaussian pulse, as shown in figure 7(*a*). Note that we used a larger control field intensity at the retrieving stage (600 μW) to increase the EIT width of the atomic medium and thereby minimize losses during release and propagation of the retrieved pulse.

The measured amplitude of the probe pulse for various storage intervals is shown in figure 7(*b*). The $1/e$ decay time of the retrieved pulse area is $\approx$500 μs (see figure 7*c*), corresponding to a decoherence rate $\approx$600 Hz, in agreement with the width of the

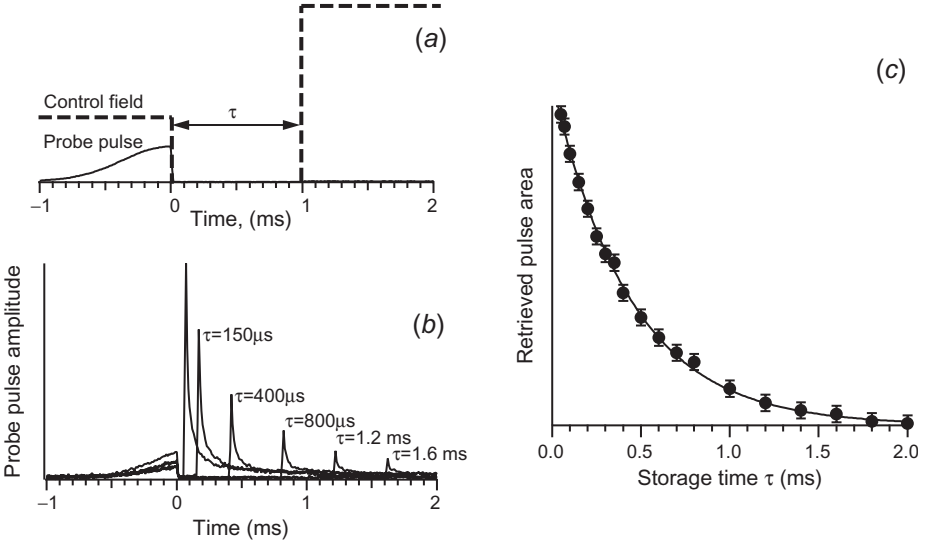

Figure 7. (*a*) Schematic of the timing and amplitude used for the probe pulse and dynamic control field in measurements of light storage as a function of storage interval τ. The control field power is 50 μW during the pulse entry stage and 600 μW during the pulse retrieval stage. (*b*) Examples of measured probe pulse storage for various storage intervals. (*c*) Retrieved pulse area as a function of storage time τ. The fitted $1/e$ decay time (solid line) is about 500 μs.

sharp central peak of the EIT resonances at low light intensity, and much narrower than the rate $1/\pi\tau_D \approx 26\,\mathrm{kHz}$ associated with diffusion of Rb atoms out of the laser beam.

The large spatial distribution of atomic coherence stored outside the laser beam allows multiple retrieved pulses to be observed by turning the control field on and off several times during the retrieval process. As a demonstration, we stored a signal pulse in the atomic ensemble; turned the control field off for 200 μs; then on for another 200 μs to retrieve a first pulse; next turned off the control field again for a variable time T; and finally turned the control field on and retrieved a second pulse. Figure 8 shows the results of these measurements and a comparison to experiments with no intermediate control field pulse. For small T, there is a large difference between the retrieved pulse areas with and without an intermediate control field application, since the second application of the control field mostly interacts with the same atoms from which coherence has already been retrieved by the first pulse. For larger values of T, however, atomic coherence diffuses back into the laser beam, and the difference between the pulses retrieved with and without an intermediate control field pulse decreases.

5. Conclusions

We have presented an initial experimental study of the effect of atomic coherence diffusion in and out of the laser beam on EIT and light storage in a Rb vapour cell with Ne buffer gas. We found that the EIT resonance lineshape is not well described by models that account for atomic diffusion with a simple homogeneous decay rate of the ground state. We also observed a sharp, narrow peak of the EIT resonance

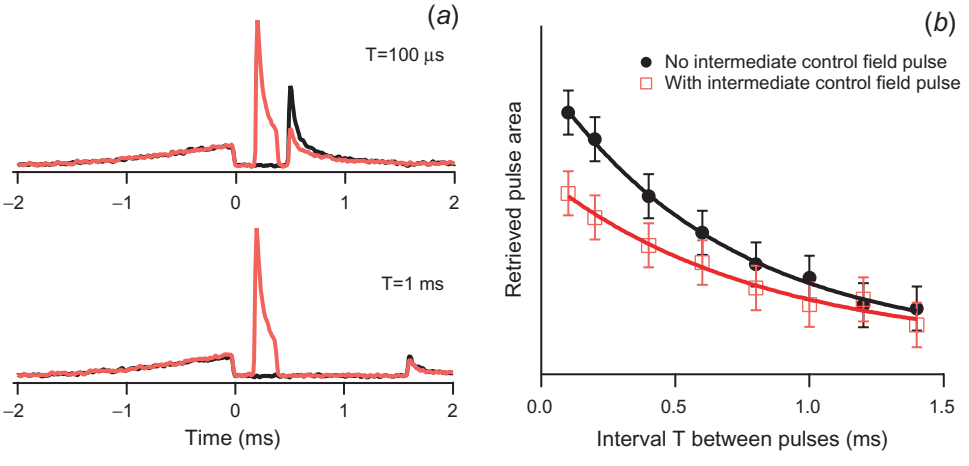

Figure 8. (*a*) Comparison between retrieved light pulses with and without an intermediate control field pulse for T= 100 μs and T= 1 ms. Control field power is 50 μW at the writing stage and 600 μW for both retrieving pulses. (*b*) Area of the retrieved probe pulses with (circles) and without (squares) an intermediate control field pulse.

that can be understood qualitatively due to the coherent atomic evolution 'in the dark' as atoms diffuse in and out of the laser beam. We found that this diffusion-induced Ramsey narrowing could be reduced by application of a suitable magnetic field gradient, $\partial B_z/\partial x$, which decoheres most atoms that diffuse out of the laser beam. We also measured light storage times consistent with the inverse of the linewidth of the narrow central peak of the EIT resonance, and observed 'replenishment' of stored light signals due to atomic coherence diffusion from the region outside of the laser beam.

Acknowledgements

The authors are grateful to F. Cané, M. Klein, C. Smallwood, M.D. Lukin, M.D. Eisaman, M. Bajcsy, L. Childress, A. André, M. Crescimanno, A. Weis, and A.S. Zibrov for useful discussions, and to Christine Y.-T. Wang for construction of the gradient coils. This work was supported by DARPA, ONR and the Smithsonian Institution.

References

[1] S.E. Harris, Phys. Today **50**(7) 36 (1997).
[2] M.O. Scully and M.S. Zubairy, *Quantum Optics* (Cambridge University Press, Cambridge, 1997).
[3] M. Fleischhauer and M.D. Lukin, Phys. Rev. A **65** 022314 (2002).
[4] M.D. Lukin, Rev. Mod. Phys. **75** 457 (2003).
[5] E. Arimondo, Phys. Rev. A **54** 2216 (1996).
[6] S. Brandt, A. Nagel, R. Wynands, *et al*., Phys. Rev. A **56** R1063 (1997).
[7] R. Wynands and A. Nagel, Appl. Phys. B **68** 1 (1998).
[8] M. Erhard and H. Helm, Phys. Rev. A **63** 043813 (2001).
[9] A. Javan, O. Kocharovskaya, H. Lee, *et al*., Phys. Rev. A **66** 013805 (2002).
[10] H. Lee, Y. Rostovtsev, C.J. Bednar, *et al*., Appl. Phys. B **76** 33 (2003).
[11] W. Happer, Rev. Mod. Phys. **44** 169 (1972).
[12] A.S. Zibrov, I. Novikova and A.B. Matsko, Opt. Lett. **26** 1311 (2001).
[13] A.S. Zibrov and A.B. Matsko, Phys. Rev. A **65** 013814 (2002).
[14] I. Novikova, A.B. Matsko and G.R. Welch, J. Opt. Soc. Am. B **22** 44 (2005).
[15] J. Vanier, J.-F. Simard and J.-S. Boulanger, Phys. Rev. A **9** 1031 (1974).
[16] F.A. Franz and C. Volk, Phys. Rev. A **14** 1711 (1976).
[17] P.T. Callaghan, *Principles of Nuclear Magnetic Resonance Microscopy* (Clarendon, Oxford, 1991).
[18] J. Jing, *Electromagnetic Analysis and Design in Magnetic Resonance Imaging* (CRC Press, Boca Raton, 1998).
[19] A.V. Taichenachev, A.M. Tumaikin, V.I. Yudin, *et al*., Phys. Rev. A **69** 024501 (2004).
[20] E. Pfleghaar, J. Wurster, S. Kanorsky, *et al*., Opt. Commun. **99** 303 (1993).
[21] R.W. Boyd and D.J. Gauthier, in *Progress in Optics*, edited by E. Wolf, Vol. 43 (Elsevier, Amsterdam, 2002), pp. 497–530.
[22] Y. Xiao, I. Novikova, *et al*., E-print archive quant-ph/0505186 (2005).
[23] I. Novikova, M. Klein, D.F. Phillips, *et al*., Proc. SPIE International Symposium on Integrated Optoelectronic Devices **5735** 87 (2005).